

Comparative secretome analysis of *Oudemansiella raphanipes* grown on different agricultural residues

Liping Zhu^{a,1}, Shunan Ma^{a,1}, Xia Gao^b, Jiandong Han^c, Weidong Lu^a, Hao Yu^{a,*}, Song Yang^{a,*}

^a Shandong Provincial Key Laboratory of Applied Mycology, School of Life Sciences, Qingdao Agricultural University, 700 Changcheng Road, Chengyang District, Qingdao 266109, Shandong Province, People's Republic of China

^b Shandong Agricultural Technology Extending Station, Jinan 250100, Shandong Province, People's Republic of China

^c State Key Laboratory of Nutrient Use and Management, Key Laboratory of Wastes Matrix Utilization, Shandong Academy of Agricultural Sciences, Jinan 250100, Shandong Province, People's Republic of China

ARTICLE INFO

Keywords:

Secretory protein
Lignocellulose degradation
CAZyme
B-Glucosidase
Laccase
MnP

ABSTRACT

Oudemansiella raphanipes can degrade lignocellulose-rich biomass, especially agricultural residues. However, its substrate utilization and degradation mechanisms remain poorly understood. To explore this, we cultured *O. raphanipes* mycelium in Kirk's liquid medium supplemented with eight distinct substrates and conducted studies on extracellular enzyme activities and secretome analysis. A total of 905 secreted proteins were identified, with the cornstalk group having the highest counts. Carbohydrate-active enzymes (CAZymes) were the predominant type (32.8–48.9 %), followed by oxidoreductases (2.8 %–13.3 %), while lipase and phosphatase were minor categories. Functional annotation of the secreted proteins comprehensively revealed their diversity in various biological processes. Among the 340 secreted proteins with Enzyme Commission codes, (Methyl) glyoxal oxidase, chitinase, and β -glucosidase were most prominent. Bran, cottonseed hulls, corncobs, and the mixture promoted mycelium growth and conserved CAZymes expression patterns. In contrast, sawdust, corn steep liquor, and cornstalk induced divergent secretome profiles. Sawdust led to a higher proportion of hemicellulose- and lignin-degrading enzymes. Corn steep liquor induced relatively high activities and abundances of laccase and MnP, while cornstalk induced a broad spectrum of oxidoreductases, lipases, and protease & peptidases. In addition, redundancy analysis further indicated that the extracellular enzyme activities (notably laccase, MnP, and xylanase) induced by different substrates significantly impacted the secretome.

Significance: *O. raphanipes* can efficiently utilize a variety of lignocellulosic materials, and genomic sequencing has confirmed the presence of abundant CAZymes in its genome. This study employed various agricultural residues as substrate inducers to elucidate the extracellular enzyme profiles of *O. raphanipes* involved in lignocellulose degradation, which indicated its metabolic plasticity in response to varying substrate composition. These findings facilitate further exploration of the biomass bioconversion mechanism of *O. raphanipes* and provide novel perspectives for the induction of combined agro-residues in its industrial cultivation.

1. Introduction

Lignocellulose, the main component of wood and agro-residues, represents the most abundant biomass available on Earth [1,2]. However, the recalcitrant structure formed by its primary constituents, cellulose, hemicellulose, and lignin, prevents the effective utilization of lignocellulose. White-rot fungi are recognized as the most efficient natural decomposers of lignocellulose [3]. Currently, agro-residues

including bran, cottonseed hulls, sawdust, bagasse, corn cobs, and rice straw, serve as indispensable nutrient sources for mushroom cultivation [4–6]. For instance, *Flammulina velutipes* can be effectively cultivated using substrates such as cottonseed hulls, corncobs, sawdust, and bagasse [7], while rice straw is a primary substrate for *Volvariella volvacea* production [8]. When *Pleurotus ostreatus* was cultivated on substrates including straw, rice, peanut leaves, and bagasse, significant differences in nutrient content were observed [9]. In the case of

* Corresponding authors.

E-mail addresses: yuhao@qau.edu.cn (H. Yu), yangsong1209@163.com (S. Yang).

¹ Liping Zhu and Shunan Ma contributed equally to this work.

P. floridar, its growth and yield exhibited a significant upward trend with the increasing content of corn husks in a medium mixed with corn husks and wood sawdust. Notably, superior yield and other biological indicators of *P. floridar* were obtained when cultivated in a medium composed of 100 % of corn husks [10]. Moreover, *Ganoderma lucidum* cultivated on bagasse exhibited more rapid mycelium growth and higher biological efficiency compared to cottonseed hulls [11]. These observations indicate that white-rot fungi display distinct substrate-specific preferences, which depend on the compositional differences in lignin, cellulose, and hemicellulose within various substrates. Different white-rot fungi also adopt diverse degradation patterns for lignocellulose. For example, *P. ostreatus*, *Coriolus versicolor*, and *Ceriporiopsis subvermisporea*, prioritize lignin degradation over cellulose, whereas *Phanerochaete chrysosporium* degrades all components simultaneously [12]. Consequently, research on the degradation of different agro-residues by white-rot fungi will facilitate the more effective utilization and biotransformation of lignocellulose.

Oudemansiella raphanipes is a widely cultivated mushroom in China with the commercial name Changgengu or Heipijizong [13]. It has gained increasing research attention in recent years due to its special flavor, high nutritional content, and pharmacological properties [13–15]. As a white-rot fungus, *O. raphanipes* possesses strong lignocellulose degrading capabilities [16,17]. Since its artificial domesticated in 1986, cultivation practices have primarily adapted methods used for *Lentinula edodes* and wood ear, relying on substrates like sawdust, cottonseed hulls, and corn cob powder with soil covering in the field for optimal yield [13]. However, there is a lack of in-depth understanding of the cultivation substrates and the relative lignocellulose degradation mechanism of *O. raphanipes*.

Fungal nutrient acquisition from lignocellulosic biomass relies on the secretion of specialized enzymes tailored to available carbon sources [18]. The lignocellulose degradation process involves complex extracellular hydrolytic systems dominated by carbohydrate-active enzymes (CAZymes) and lignin-modification enzymes (LMEs) [19–21]. Substrate type and complexity significantly influence the secretome profiles, thereby impacting fungal growth and development [22,23]. The diverse strategies for lignocellulose degradation could be reflected in the differences among the secretomes, making comparative secretomic analysis a powerful tool to detect the enzyme composition, degradation step coordination (interactions and synergies), and novel enzyme discovery [24–26]. Recently, secretomic studies on white-rot fungi such as *L. edodes*, *Morchella importuna*, *P. ostreatus*, *P. eryngii*, *Agaricus bisporus*, etc, have been widely conducted [23,27–30]. However, these investigations primarily focused on 1–3 common agro-residues (e.g. sawdust, bagasse, rice straw) and lacked comprehensive comparisons across diverse substrates. Current research on *O. raphanipes* is limited to individual cellulose- or lignin-degrading enzymes involved in lignocellulose degradation, with no systematic analysis of its enzyme induction profiles or degradation patterns under different substrates. Therefore, exploring the effects of a broader range of agro-residues on secreted enzyme profiles of *O. raphanipes* is critical.

Our previous complete genome sequencing of *O. raphanipes* revealed its rich repertoire of lignocellulolytic enzymes [17]. Integrating secretomic analysis with genomic information can provide critical insight into the extracellular enzyme systems involved in substrate degradation. The mycelial growth phase was selected due to its crucial role in lignocellulose breakdown [31]. Here, we evaluated *O. raphanipes* mycelia growth and extracellular enzyme activities of laccase, manganese peroxidase, cellulase, xylanase, and amylase in culture supernatants across eight agro-residues-based media, followed by comparative secretome profiling. This investigation represents the first comprehensive characterization of *O. raphanipes* extracellular enzyme profiles induced by diverse agro-residues, aiming to elucidate its lignocellulose degradation mechanisms and provide secretomic insights for optimizing cultivation substrates.

2. Materials and methods

2.1. Organisms and inoculum preparation

The Basidiomycete strain *O. raphanipes* CGG-1 used in this study was provided by the Shandong Provincial Key Laboratory of Applied Mycology. Its genome was formerly sequenced and deposited in the Genome Warehouse of the National Genomics Data Center (accession number GWHBRAH00000000 and GWHBRAI00000000 for two monokaryons) [17]. This fungal strain was preserved on potato dextrose agar (PDA) slants and stored at 4 °C, with regular reactivation for maintenance. For the preparation of fungal inoculants, the strain was cultivated in 500 mL flasks containing 200 mL of the following potato dextrose broth (PDB) nutrient medium at 25 °C. The pH of the medium remained natural after sterilization at 121 °C for 20 min. After culturing the fungi for 14 days, the mycelium pellets were collected. The residual culture matrix was washed away with sterile water 2–3 times, and the mycelium was homogenized using sterilized glass beads. The sample was snap-frozen in liquid nitrogen and subsequently stored at –80 °C. Samples were collected in triplication for each treatment.

2.2. Cultivation conditions

The glucose-free Kirk's liquid medium, containing 9 mmol/L KH_2PO_4 , 3 mmol/L $\text{MgSO}_4 \cdot 7\text{H}_2\text{O}$, 0.02 mmol/L ammonium tartrate, 0.3 mmol/L $\text{CaCl}_2 \cdot 2\text{H}_2\text{O}$, and 10 mL/L trace element, was selected as the standard culture medium [32]. To elucidate the effect of different carbon inducer sources on the secretory enzyme activities of *O. raphanipes* CGG-1, an equal amount (40 g/L) of different dried agricultural biomass substrates, including bran, cottonseed hull, corncob, cornstalk, corn steep, basswood sawdust, and a mixture (with each component mixed in equal proportions), were added individually as substrate carbon sources. This dried matrix was crushed into 1–2 mm pieces. Additionally, controls with only the addition of 10 g/L of carboxymethyl cellulose (CMC) were run in parallel. The samples cultured on corresponding substrates were designated as follows: the bran group (Bran), the cottonseed hull group (CH), the corncob group (CC), the corn steep liquor group (CSL), the cornstalk group (CSK), the sawdust group (SD), the mixture group (Mix), and CMC group. All experiments were conducted with three replicates. The pH of the medium remained natural after sterilization for 30 min at 121 °C. Approximately 3 mL of homogenized fungus was inoculated into 250 mL flasks and then incubated at 25 °C. Throughout a 30-day incubation period, the supernatant was collected at five-day intervals and then centrifuged at 10,000 $\times g$ for 5 min. The activities of laccase, manganese peroxidase, cellulase, xylanase, and amylase in the supernatant were subsequently determined. At the end of the cultivation, the mycelia of each sample were collected and measured in dry weight. The protein content of the mycelium and the supernatant on the 15th day was measured using the modified BCA protein assay kit (Sangon Biotech).

2.3. Enzyme assay

2.3.1. Laccase

Laccase activity was determined by the oxidation of 2,2-Azino-bis-3-benzothiazole-6-sulfonic acid (ABTS) method [28]. The standard reaction mixture contained 190 μL of 1 mM ABTS ($\epsilon_{420} = 3.60 \times 10^4 \text{ M}^{-1} \cdot \text{L} \cdot \text{cm}^{-1}$) in substrate buffer (50 mM sodium propionate buffer, pH 4.5) and 10 μL of enzyme solution. Laccase activity was calculated from the optical density changes at 420 nm measured every 5 min. One unit (U) of enzyme activity was defined as the amount of the laccase that oxidized 1 μmol of ABTS substrate per minute. Enzyme yield was expressed as U/mL.

2.3.2. Manganese peroxidase (MnP)

MnP activity was determined by detecting the formation of Mn^{3+}

malonate complex at 468 nm in the detection buffer containing 50 mM sodium propionate buffer (pH 4.5), 1.0 mM 2, 6-dimethylphenol (2, 6-DMP, $\epsilon_{468} = 4.96 \times 10^4 \text{ M}^{-1} \cdot \text{L} \cdot \text{cm}^{-1}$), 1.0 mM MnSO_4 , and 0.1 mM H_2O_2 [33]. A 10 μL enzyme solution sample was incubated in 190 μL substrate solution. One unit of MnP activity was defined as the amount of enzyme that oxidized 1 μmol of 2, 6-DMP per minute. Enzyme yield was expressed as U/mL.

2.3.3. Cellulase, xylanase and amylase

The endoglucanase activity was employed to evaluate the cellulase enzyme activity. The measurement of the cellulase, xylanase, and amylase activities was performed using a modified DNS assay method [34–36]. In the preparation stage, 1 % of each substrate (sodium carboxymethyl cellulose for cellulase, xylan for xylanase, and soluble starch for amylase) was mixed into 0.05 M sodium citrate buffer (pH 5.0). The 1 % DNS solution, was prepared a week in advance and stored in brown bottles. For the reaction, 1.0 mL of substrate solution was mixed with 1.0 mL of enzyme solution (while using an equal volume of culture medium without enzyme as the control), and then the reaction mixture was incubated at 50 °C for 30 min. Subsequently, 2 mL of 1 % DNS solution was added, and the mixture was then heated at 100 °C for 5 min before cooling the tubes on ice and measuring the absorbance at 540 nm. The reduced sugar content was calculated using a standard curve. The definition of one unit of enzyme activity is the amount of enzyme required to release 1 μg of reducing sugar (xylose for xylanase; glucose for cellulase and amylase) per minute in the assay condition. The enzyme yield was reported in units per mL (U/mL).

2.4. Secretory proteomic analysis

After 14 days of cultivation, the culture was filtered using 6-layer absorbent cotton gauze. The filters were then centrifuged at 8000 rpm for 20 min. The resulting supernatant was collected and subjected to secreted protein extraction using phenol extraction coupled with ammonium acetate precipitation as previously described [37]. Protein pellets were re-dissolved in a 4 % SDS buffer (in 100 mM Tris-HCl buffer, pH 7.6) and digested using trypsin according to the STrap methods [38]. LC-MS/MS analysis of peptides was performed using an EASY-Nano system coupled with Orbitrap Fusion™ Tribrid™ detectors (Thermo Fisher, USA) [39]. Three biological replicates were performed for each group.

2.5. Identification and bioinformatic analysis of proteins

The MS raw data of each sample were combined and searched using Proteome Discoverer software suite version 2.0 (Thermo Fisher Scientific, San Jose, CA, USA) against the *O. raphanipes* proteome database (proteome ID UP000076154) from UniProt. Protein identification was supported by at least two unique peptides with a false discovery rate lower than 0.05. Raw data obtained from Proteome Discovery software was normalized as follows. Firstly, missing values were supplemented (three sets of data, data with only one set was deleted, and missing values in data with two or three sets were supplemented, which is the k-proximity method). Then, median standardization was executed on intensity data. CNSknowall was used to construct Venn diagrams. (<http://cnsknowall.com/>). Kyoto Encyclopedia of Genes and Genomes (KEGG) [40] (<http://www.kegg.jp/> (accessed on 15 Dec 2024)) databases were utilized to analyze the functional annotations and metabolic pathways of differentially abundant proteins. Enrichment diagrams of KEGG pathway annotations were generated using OmicShare online tools (<https://www.omicshare.com/tools>). DbCAN for carbohydrate-active enzyme (CAZyme) families (based on CAZyDB07/15/2016) was used to annotate the identified proteins. The presence or absence of a signal peptide was predicted with SignalP 4.1 [41].

2.6. Statistical analysis

The results of the enzyme activities are represented as the mean \pm SD (standard deviation) values from three replicates. These means were subjected to a comparison using a one-way analysis of ANOVA with the Duncan test conducted subsequently to evaluate the effect of different inducer sources on the enzyme production by *O. raphanipes*. Statistical significance was set at $p < 0.05$. The data were analyzed using GraphPad Prism 8.0 software. The error bars in all figures indicated the SD of three replicate values for each treatment. Before performing the ANOVA, the homogeneity of variances was confirmed by Levene's test, which showed no significant difference when $p > 0.05$. Redundancy analysis (RDA) to evaluate the relationship between enzyme activities and the CAZymes expression abundance, was performed using the online tool at www.bioincloud.tech/standalone-task-ui/rda. The raw data for the secretome in this paper has been deposited in the OMIX with the accession number OMIX008748.

3. Results

3.1. The growth of *O. raphanipes* mycelia in liquid media supplemented with different substrates

Mycelial pellets of *O. raphanipes* were inoculated into Kirk's liquid media supplemented with different agro-residues as carbon inducers and cultivated statically at room temperature in darkness. Significant differences in the mycelial growth under various conditions were observed on the 7th day (Fig. 1). As depicted in Fig. 1a, media containing bran, cottonseed hulls, or the mixture, supported extremely luxuriant growth, with dense mycelial mats covering the liquid surface and forming uniform, thick aggregates at the bottom. This vigorous growth could be attributed to relatively high cellulose content in bran and cottonseed hulls [42]. In contrast, corn steep liquor-supplemented medium exhibited the lowest surface coverage but a higher dry weight with a dense and thick mycelial mat (Fig. 1a and b). This was probably due to submerged growth patterns rather than surface colonization caused by the absence of a solid matrix. Next, media containing corn-stalks or basswood sawdust (with relatively high lignin content) exhibited intermediate growth, characterized by thin and loose mycelial layers and low mycelial dry weight. CMC-supplemented medium showed minimal growth with no mycelial layer or mat formed. Moreover, protein quantification on the 15th day revealed that mycelial protein content was positively correlated to a certain degree with mycelial growth and dry weight (Fig. 1c). Bran-supplemented medium exhibited the highest mycelial protein content and extracellular protein production, followed by corn steep liquor medium (Fig. 1c and d). This correlated with their roles as carbon-source inducers and nitrogen sources [43]. Overall, *O. raphanipes* can effectively utilize bran, cottonseed hulls, and corn steep liquor to promote early-stage mycelial growth.

3.2. Effects of different carbon inducers on enzymatic activity of *O. raphanipes*

During the mycelial culture period, samples were taken from different media every five days to determine the activities of enzymes. It was found that almost all enzyme activities reached the highest on the 20th ~ 25th day (Fig. 2). As illustrated in Fig. 2a and b, the CSL group had a significant advantage in the activities of laccase and MnP. In contrast, the activities of other groups, especially the SD and CH groups, were quite low, while the CSK group showed a small peak on the 20th day. The Bran and CH groups exhibited a high level of CMCCase activity, while the CMC and the Mix groups showed high xylanase activity (Fig. 2c and d). Also, the CMC group showed a high CMCCase activity only at the initial stage. Besides, the Bran and CC groups showed moderate xylanase activity, and the others remained extremely low throughout

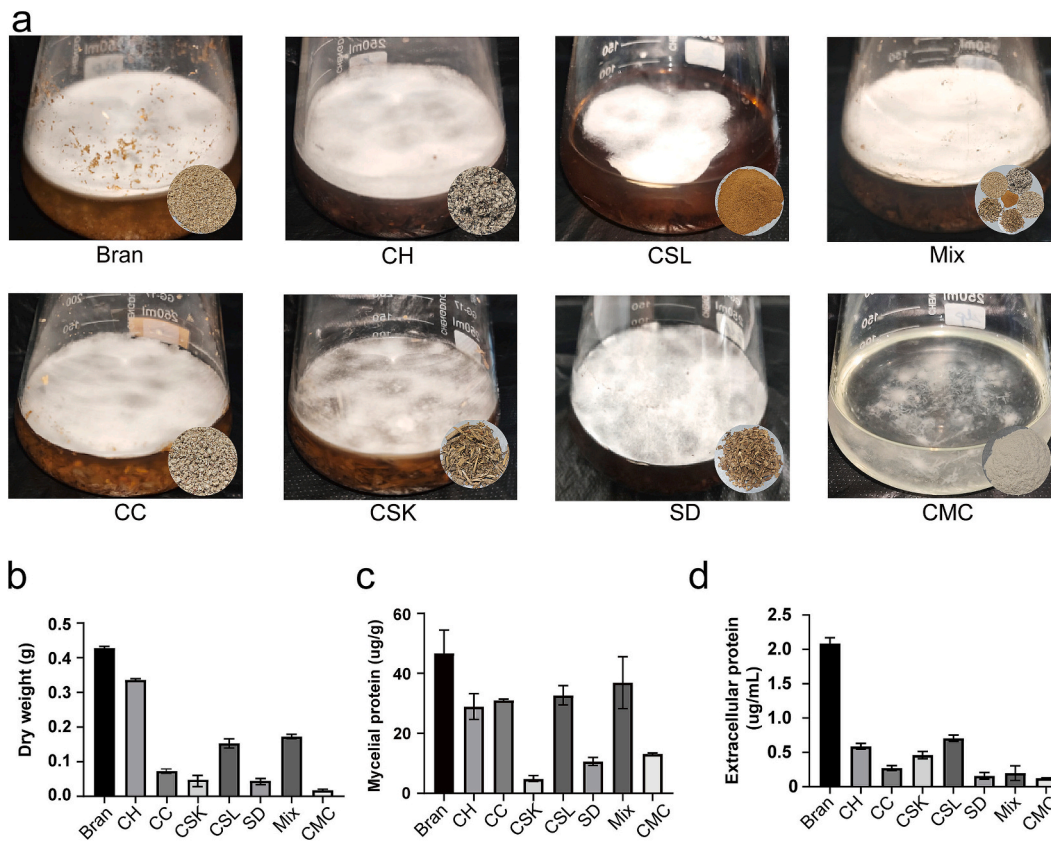


Fig. 1. Morphology and physiology of *O. raphanipes* mycelium. (a) The growth of mycelium during the static culture in different substrates as well as the mycelium dry weight, (b) protein content of the mycelium, (c) and the extracellular protein content. (d) The annotations below indicate the addition of different substrates: Bran, for bran; CH, for cottonseed hull; CC, for corncob; CSK, for cornstalk; CSL, for corn steep liquor; SD, for sawdust; Mix, for the mixture; CMC, for carboxymethyl cellulose.

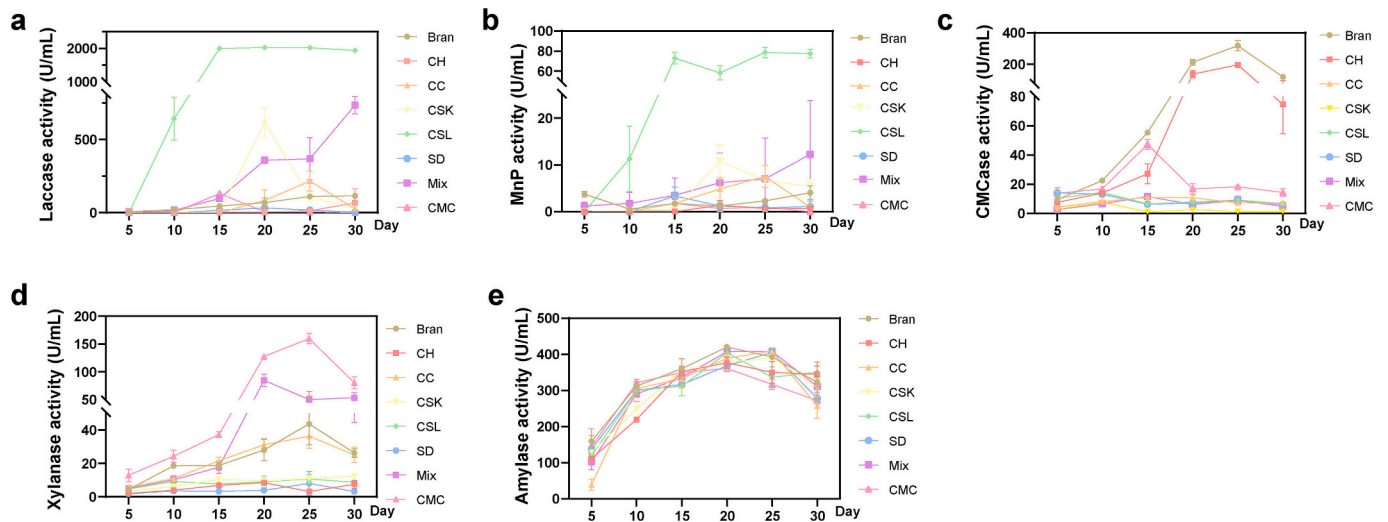


Fig. 2. Enzyme activities of *O. raphanipes* during continuous culture in different media. (a) Laccase activity, (b) MnP activity, (c) CMCase activity, (d) Xylanase activity, and (e) Amylase activity.

the entire cultivation period. The amylase activity showed high levels from the initial stage of the cultivation (the 5th day), with no significant difference among the various groups, though the Bran group had a slight advantage (Fig. 2e). These results indicated the strong ability of *O. raphanipes* to induce the production of cellulose-, xylan-, and starch-degrading enzymes by the bran, and to induce laccase and MnP activity by the corn steep liquor. The CMC demonstrated a moderate capacity to

induce activities of cellulase and xylanase but quite low activities of laccase and MnP. However, the sawdust had the lowest ability to induce the activity of all these enzymes.

3.3. Secretome profiles of *O. raphanipes* cultured in media with different carbon inducers

Changes in enzyme activities reflect the metabolic responses of *O. raphanipes* to diverse carbon-source inducers and are dictated by the overall secretome composition. Variations in enzyme activities across different groups are likely due to the differential secretion of protein types and abundances, affecting the secretome profile. To characterize these dynamics, quantitative label-free proteomics was applied to analyze the secretome of *O. raphanipes* during mycelial growth. Most proteomic analyses of animal tissues, cells, and bacteria use simple buffers for protein extraction, such as Tris-HCl buffer and urea-based buffer [44]. However, the existence of macromolecules in the cell wall can influence protein extraction efficiency and enzymatic digestion. Therefore, we used a combination of phenol extraction and ammonium acetate precipitation for protein extraction, a method that generates a relatively low amount of contaminating compounds and has proven to be simple and efficient [37]. Subsequently, LC-MS/MS analysis with high sensitivity and high throughput was conducted, enabling us to identify and quantify the secretome proteins accurately [45].

A total of 905 secreted proteins were identified, including 537, 481, 487, 440, 661, 442, 456, and 467 proteins identified in the Bran, CH, CC, CSL, CSK, SD, Mix, and CMC groups, respectively (Fig. 3a). Among them, 215 shared proteins were found across all groups. The CSK group had the highest number of identified proteins, with the highest number of unique proteins at 153. The number of unique proteins expressed in other groups was relatively lower, with the CMC group showing the most (21 proteins), while the Mix group had no uniquely secreted proteins. Nearly 57 % of the total detected proteins (517/905) contain a predicted signal peptide and 94 transmembrane (TM) proteins were computed in the secretomes (Supplemental Table 3).

The abundance of these secreted proteases is critically affected by the substrate composition. Principal component analysis (PCA) results revealed that samples within the same group clustered together, while those from different groups were divided into five distinct clusters by the first and the second components (Fig. 3b). Among them, the CMC group was significantly separated from the other groups. The CSK group, having the largest number of proteins, was found to be close to the CH group, indicating similar protein expression patterns. Notably, the CSL group and SD group were separated from each other as well as from the other groups, indicating that the texture component of these two agro-residues was distinct from others. Additionally, the Bran, CC, and Mix groups exhibited a higher degree of similarity, with the Mix group showing a particularly close association with the Bran group, which

suggested that the inclusion of corncob and bran in the mixture had a predominant influence on the mycelial protein secretion of *O. raphanipes*. Pearson correlation coefficient analysis showed similar results (Fig. 3c).

3.4. Functional annotation of the secreted proteins

The secreted proteins were classified into the following types according to their functions: CAZyme, oxidoreductase, lipase, phosphatase, protease & peptidase, and other proteins [23]. The statistics of the quantities of these types in each group are shown in Fig. 4a. Across all groups, CAZymes were the most prevalent proteins identified in the secretomes, ranging from 32.8 % (CSK group) to 48.9 % (SD group) of the total proteins. In addition, the CSK group displayed the largest amount of oxidoreductase, protease, and peptidase among all groups. According to KEGG annotation, the secreted proteins were mainly involved in “Global and overview maps”, “Carbohydrate metabolism”, “Amino acid metabolism”, “Translation”, and “lipid metabolism” (Fig. 4b). A more in-depth analysis was conducted on the top 20 pathways (Fig. 4c), which showed that these pathways were predominantly engaged in the metabolic pathways (ko01100), the secondary metabolites biosynthetic pathways (ko01110), carbon metabolism (ko01200), starch and sucrose metabolism (ko00500), Glycolysis / Gluconeogenesis (ko00010), and ribosomal pathways (ko03010). Of these secreted proteins, 340 were assigned Enzyme Commission (EC) codes (Table S2). The protein with the highest abundance was EC1.2.3.15 ((Methyl) glyoxal oxidase), followed by EC3.2.1.14 (Chitinase), EC3.4.25.1 (Proteasome endopeptidase complex), EC3.2.1.21 (Beta-glucosidase), EC4.2.2.2 (Pectate lyase), EC3.4.14.9 (Tripeptidyl-peptidase I), and EC3.2.1.19 (Heparinase). They were mainly involved in pathways such as ko00520 (Amino sugar and nucleotide sugar metabolism), ko00460 (Cyanoamino acid metabolism), ko00500, ko00040 (Pentose and glucuronate interconversions), and ko01100. This functional annotation comprehensively reveals the diverse functions of the secreted proteins in various biological processes.

3.5. Analysis of the CAZymes between different Secretomes

The CAZyme family plays a critical role in complex carbohydrate metabolism as well as many other important physiological processes, such as the breakdown of plant cell walls and the metabolism of complex polysaccharides [38]. Across the eight groups studied, CAZyme was the most abundant enzyme, ranging from 32.8 % in the CSK group to 48.9 % in the SD group. A total of 302 CAZyme proteins were identified from all

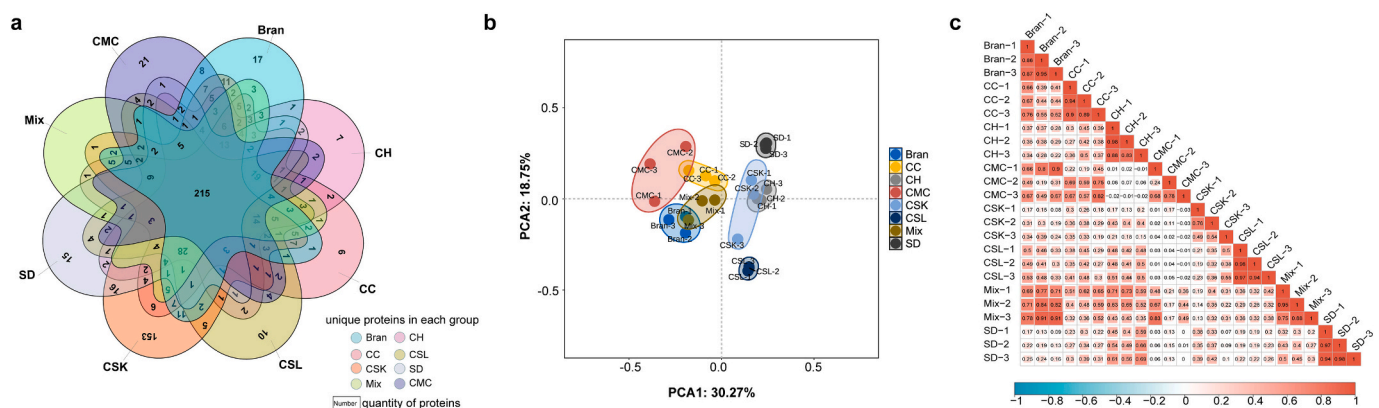


Fig. 3. Statistics of the secretome data of *O. raphanipes* samples cultivated on different carbon substrates. (a) Venn diagram of proteins in the secretome of different groups. The unique proteins of each group and the shared proteins among groups are depicted with numbers, which represent the quantity of proteins in that particular category. The 215 common proteins shared by all groups are shown in the middle. (b) Principal component analysis (PCA) for secretome data of different groups. PCA was conducted with parameters as follows: method is normalize and the confidence region is set to 95 %. (c) Pearson correlation coefficient (PCC) analysis of secretome data between each group with the corresponding coefficient values marked. Each group was treated with the corresponding substrate with three repeats marked as -1, -2, and -3.

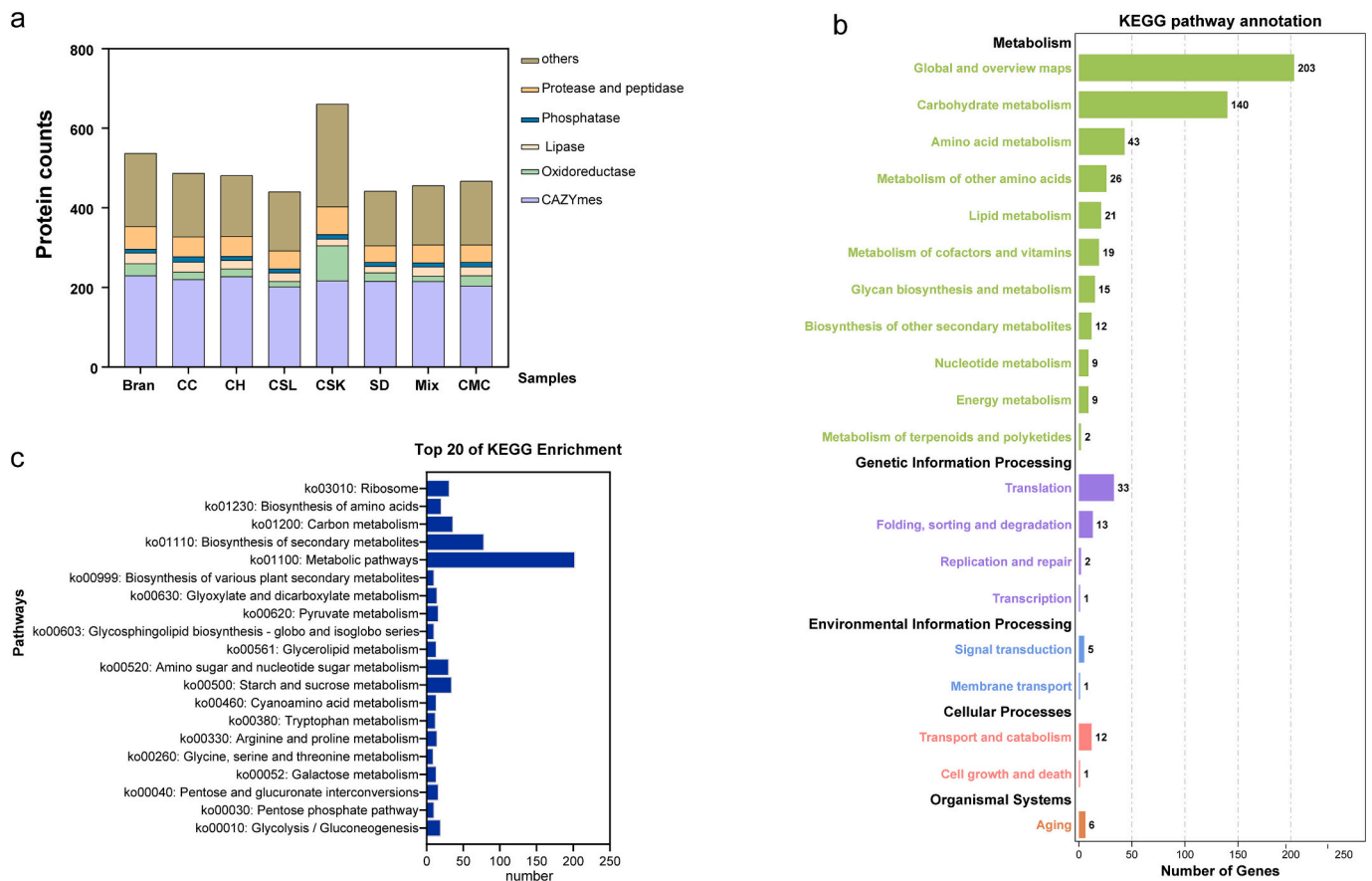


Fig. 4. Functional analysis of the secretome proteins. (a) Quantitative display of different types of secreted proteins in each group: Bran, for bran; CH, for cottonseed hull; CC, for corncob; CSK, for cornstalk; CSL, for corn steep liquor; SD, for sawdust; Mix, for the mixture; CMC, for carboxymethyl cellulose. Columns in different colors indicate the relative types of the secreted proteins. (b) Distribution of enriched KEGG for all the secreted proteins. The vertical axis represents the five primary pathway types, including Metabolism, Genetic Information Processing, Environmental Information Processing, Cellular Processing, and Organismal Systems. Each bar represents the secondary pathway type, with the number indicating the quantity of relevant proteins enriched in each secondary pathway. (c) Top 20 enriched KEGG pathways of all the secreted proteins. The vertical axis represents the top 20 pathways and the horizontal axis indicates the quantity of the proteins enriched in this pathway.

groups, including 164 glycoside hydrolases (GHs), 20 polysaccharide lyases (PLs), carbohydrate esterases (CEs), 89 auxiliary activities (AAs), and 5 carbohydrate-binding modules (CBMs). The specific distribution of these CAZymes in each group was shown in Fig. 5a. Some of the most important CAZymes (GH3, GH6, GH7, GH10, GH35, GH43, GH51, 1CE, 2CE, 4CE, PL1, AA3, AA5, AA7, and AA9) were secreted in almost all groups, suggesting their essential roles in biomass degradation (Table S3). Functionally, the CAZyme family can be further divided into cellulase, hemicellulase, lignin-degrading protein, pectinase, amylase, other polysaccharide-degrading protein, cell wall remodeling protein, and chitinase [23]. The main proteins within these functional enzyme categories and their expression levels in each group were shown in Table S3. Overall, certain enzymes related to the degradation of cellulose, hemicellulose, and lignin degradation, showed significantly high expression levels in each group, whereas those of pectinase and esterase were relatively low across all groups. Furthermore, an in-depth analysis was conducted to investigate the differential protein expression profiles among various comparisons (Fig. 5b and Fig. S1). Specifically, in this study, these comparisons were obtained by comparing each of the other groups against the CMC group. The CSL group was separated from the other comparisons and the SD group clustered closely with the CSK group. The Mix group showed a closer relationship with the CC, CH, and Bran groups (Fig. 5b).

For cellulose degradation enzymes, according to the clustered heatmap analysis, the CSL group was significantly different from other groups, and the Mix group was closest to the CC and CH groups

(Fig. S1a). Enzymes belonging to the representative GH3 family had relatively high expression levels in the CH and Mix groups. In contrast, the GH6 (MDBOrad1_15394) and GH7 (MDBOrad1_05282) families (belonging to cellobiohydrolase), GH10 (MDBOrad1_06259, related to Endo-1,4-beta-xylanase), as well as AA9 (MDBOrad1_02063, belong to endo-beta-1,4-glucanase D) were significantly downregulated in all the comparisons. This indicated that these enzymes achieved comprehensively high expression abundance in the CMC group (Fig. S1a). Regarding hemicellulose degradation, the Bran and CSL groups clustered together and were separated from other groups (Fig. S1b). Additionally, the Mix group clustered with the CSK group, indicating a similarity between these two groups in terms of hemicellulose degradation. Representative families such as GH27, GH35, and GH51 showed a high level of upregulated expression in all comparisons, while the enzymes from GH45 and GH43 families exhibited an obvious downregulated expression. As for the expression of lignin-degrading enzymes, based on the clustered heatmap analysis, the SD group was remarkably separated from the other groups, while the CH group and the Mix group were relatively close to the CSL group and the CC group, respectively (Fig. S1c). Approximately one-third of the representative enzymes from the AA1, AA3, AA5, and AA7 families were upregulated in all comparisons, while about half of them were downregulated. Among these, MDBOrad1_11676 (AA3) and MDBOrad1_13266 (AA7), were significantly downregulated in the CH, CSL, and CC groups when compared to the CMC group (Fig. S1c). The analysis of the pectinase- and esterase-related enzymes also revealed that the SD group differed from the

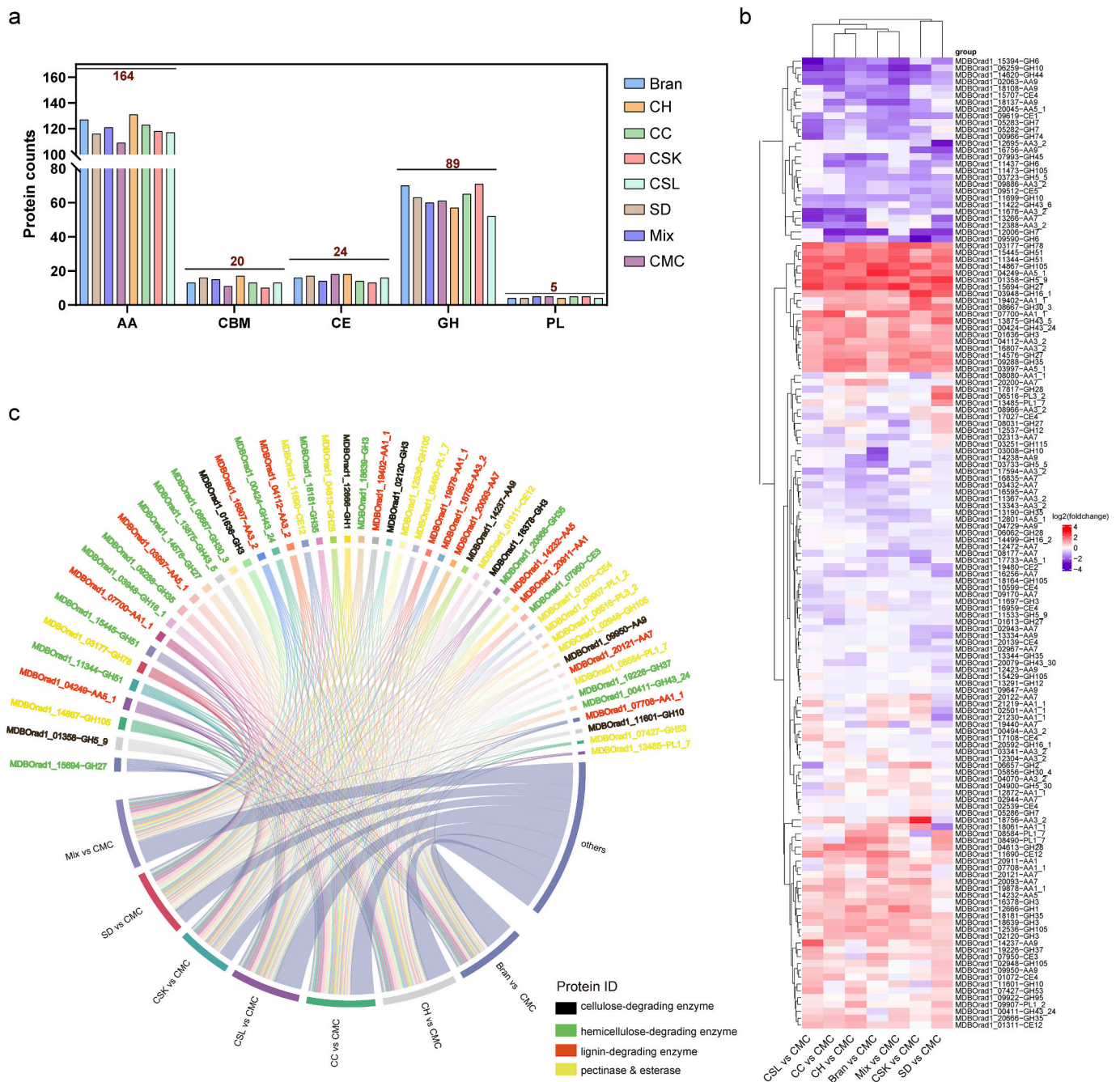


Fig. 5. Functional classification of CAZymes. (a) Quantity and classification of CAZymes induced by different substrates. GH, glycoside hydrolases; PL, polysaccharide; CE, carbohydrate esterases; AA, auxiliary activities; CBM, carbohydrate-binding modules. (b) Heatmap of the differential protein expression of the CAZymes among the comparisons. The heatmaps display the log₂(foldchange) of protein abundance in various comparisons, where each group is separately compared to the CMC group. Each row corresponds to a specific protein. (c) The chord diagram displays the top 50 differential proteins. The colors and symbolic attributes of the protein IDs are shown in the legend.

other groups (Fig. S1d). Above all, it was evident that CAZymes in the CMC group were mainly associated with cellulose degradation. The Mix group clustered with different groups (including the CH, CSK, CC, and Bran groups), depending on different functional enzymes. This illustrated the tendency of different substrates in the Mix group to trigger the production of related enzymes. The top 50 proteins with significant differences among the comparisons were displayed in Fig. 5c. Among them, enzymes related to hemicellulose degradation and lignin degradation account for the major portion.

3.6. Analysis of the expression of other secreted proteins between different groups

In this study, other types of secretome proteins, including oxidoreductase, phosphatase, lipase, and protease & peptidase were identified as illustrated in Table S4. The CSK group showed the largest number of proteins related to oxidoreductase and protease & peptidase (Fig. 4a). Subsequently, all groups were contrasted with the CMC group, to analyze the differential protein levels of each comparison. Clustered heatmap analysis revealed that the protein expression pattern in the CSK group was significantly distinct from that of the other groups (Fig. 6),

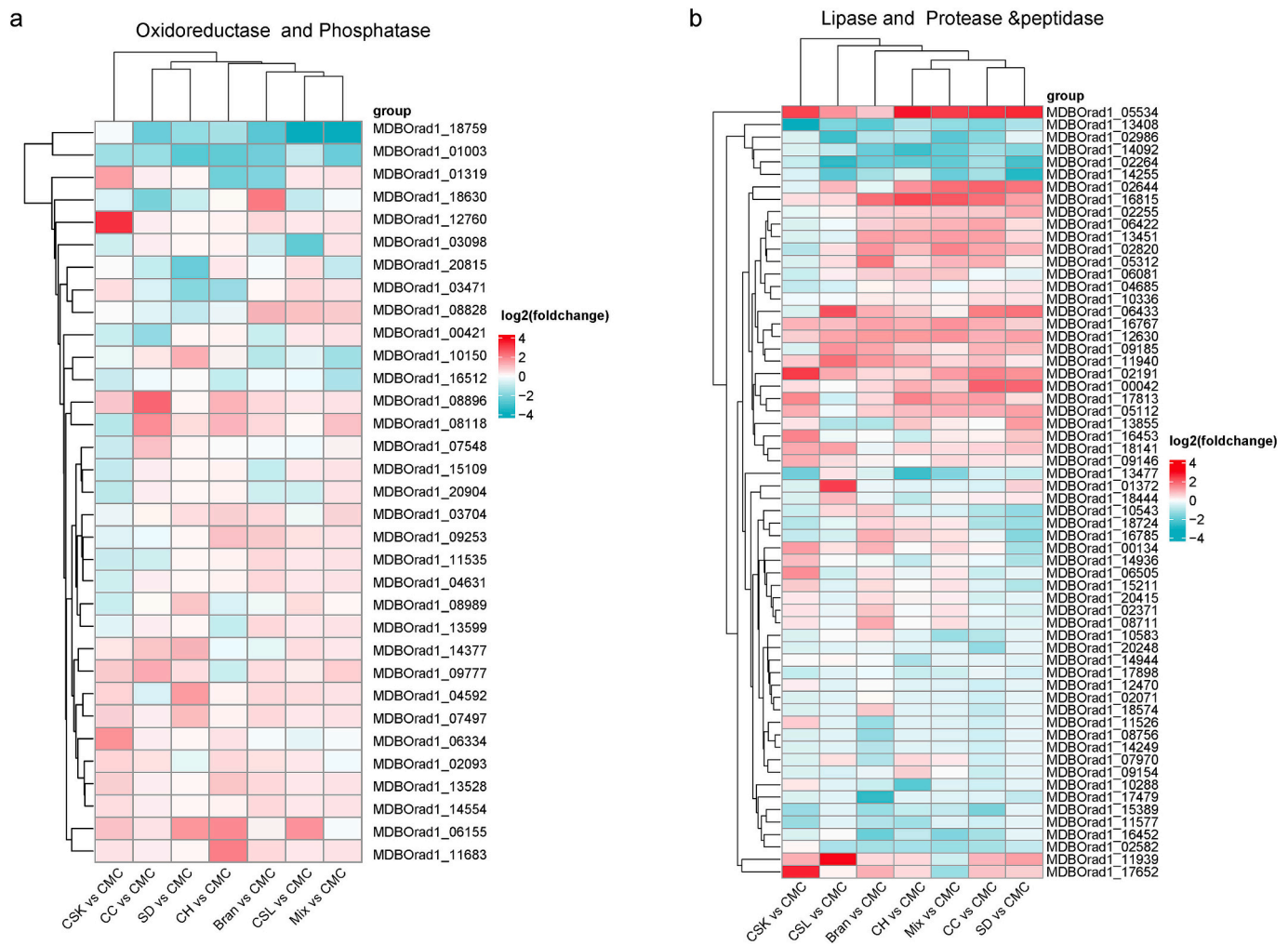


Fig. 6. Heatmap of other types of secretomic proteins. (a) Proteins related to oxidoreductase and phosphatase. (b) Proteins related to lipase and protease & peptidase.

The heatmaps display the $\log_2(\text{foldchange})$ of protein abundance for different comparisons, with red indicating the up-regulation and green indicating the down-regulation. (For interpretation of the references to colour in this figure legend, the reader is referred to the web version of this article.)

indicating the unique and diverse secreted proteins induced by cornstalks. In addition, the CSK vs CMC comparison showed the largest number of down-regulated proteins. Regarding oxidoreductase- and phosphatase-related proteins, the SD and CC groups clustered in proximity. Similarly, the CSL and Mix groups were also closely clustered (Fig. 6a). As for lipase and protease & peptidase-related proteins, the SD and CC groups, along with the CH and Mix groups, were significantly clustered together (Fig. 6b). It was evident that the SD and CC groups were the most proximate, whereas the other four groups, Bran, CH, CSL, and Mix, were relatively close to one another. Among them, the Mix group was comparable to the CSL group in terms of oxidoreductase and phosphatase, while it resembled the CH group in terms of protease & peptidase.

3.7. Relationships between extracellular enzyme activity and the expression abundance of CAZymes in the Secretome

Redundancy analysis (RDA) showed a correlation between the extracellular enzyme activity and the protein expression of the related CAZymes (Fig. 7). The extracellular enzyme activity on the first ordination axis accounted for 23.89 % of the observed variations, and the second ordination axis explained 19.32 %. Regarding the expression of CAZyme proteins, the CMCCase activity, represented by the shortest line, had the least impact on the secretome compared to other enzyme

activities. A positive correlation was evident between the cornstalk substrate and CMCCase activity, as well as between the CMC substrate and xylanase activity. Key enzymes contributing to these two extracellular enzymes activities included GH6 (MDBOrad_15394), GH10 (MDBOrad_11699), GH152 (MDBOrad_20668), and CBM67 (MDBOrad_13561). In contrast, the corn steep liquor or bran substrate exhibited a positive correlation with MnP, laccase, amylase, and extracellular protein content, with enzymes mainly involved were those related to AA1 family, such as MDBOrad_21219, MDBOrad_19878, MDBOrad_21230. However, the cottonseed hull or sawdust substrate was negatively correlated with all these enzyme activities.

4. Discussion

Lignocellulose is a highly variable and complex biomaterial composed of cellulose, hemicellulose, lignin, and pectin [46–48]. Fungal secretome proteins, consisting of a wide variety of extracellular enzymes and active metabolites, play a crucial role in lignocellulose degradation [28]. Previous research on cultivating *Oudemansiella* strains on various lignocellulosic substrates underscored their ability to produce lignocellulosic enzymes, essential for material decomposition and mycelial growth [49,50]. This study investigated the secretome proteins of *O. raphanipes* cultured on diverse agro-residues as substrates. To evaluate the degradation capabilities of *O. raphanipes* regarding different

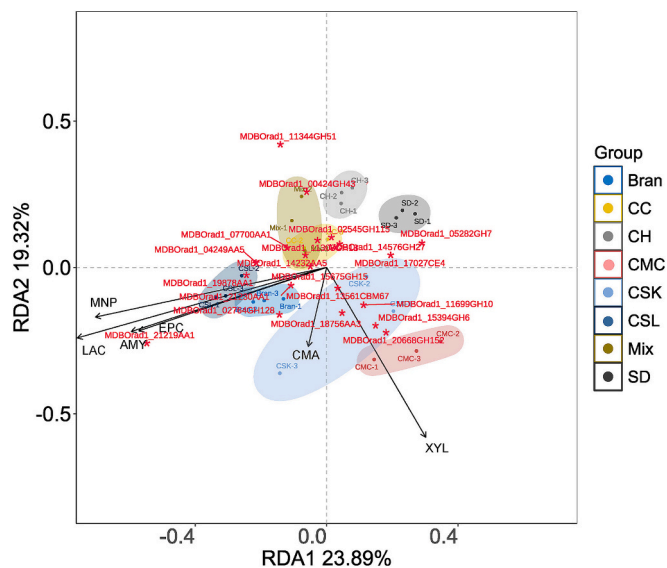


Fig. 7. Redundancy analysis of the indicated enzyme activity and the expression of the CAZymes related to lignocellulose degradation. The arrow length represents the intensity of the enzyme activity influence on CAZymes of the secretome. The angle between the arrow and the axis represents the correlation between the indicated enzymes and the axis; smaller angles correspond to higher correlations. The distance between each sample point and arrow indicates the strength of the effect of the indicated enzymes on the sample. The asterisks represent the dominant proteins of the CAZymes. CMA, CMCCase; AMY, amylase; LAC, laccase; MNP, manganese peroxidase; XYL, xylanase; EPC, extracellular protein content.

culture substrates, the abundances of the secretome proteins derived from the substrates of bran, cottonseed hull, corncob, cornstalk, corn steep liquor, sawdust, the mixture, and CMC were respectively exhibited (Fig. S2).

4.1. Cellulose-degrading ability

White-rot fungi depolymerize crystalline cellulose with the aid of lytic polysaccharide monoxygenases (LPMO, AA9 family) [51]. Subsequently, cellobiohydrolases (GH6 and GH7), endoglucanases (GH5, GH9, GH12, GH44 and GH45), endo-1,4- β -xylanases (GH10), as well as β -glucosidases (GH1 and GH3) fully digest the depolymerized cellulose. Generally, the efficient degradation of cellulose requires synergistic cooperation of cellobiohydrolases and endoglucanases [52]. In the secretome of *O. raphanipes*, two LPMO proteins (MDBOrad1_09950 and MDBOrad1_13334) were identified. MDBOrad1_09950 had a relatively high expression in the SD and CSL groups, and MDBOrad1_13334 was only expressed in the CSK, SD, and CMC groups. However, the SD group showed extremely low CMCCase activity, indicating rate-limiting steps in other cellulose-degrading enzyme activities (Fig. 2c and S2a). In contrast, high CMCCase activity was observed in the Bran, CH, and CMC groups, the first two of which were clustered together regarding the expression analysis of all cellulose-degrading enzymes (Fig. S2a). This was consistent with the results reported in other fungi, such as *L. edodes*, *P. chrysosporium*, and *P. ostreatus* [53], where rice bran was proved to be the best inducer of cellulase activity, and CMC and xylose were also effective [54]. Among these three groups, the Bran and CH groups showed an advantage in expressing GH3-family enzymes, while the CMC group had relatively high expression of GH6, GH7, and GH10 families. This implies the diversity and complexity of the cellulose degradation patterns in *O. raphanipes*. Notably, the GH6 and GH7 families, which belong to cellobiohydrolase, are responsible for degrading crystalline cellulose in most of the cellulolytic systems [52]. The high abundance of these two families may be the reason for the relatively high CMCCase

activity in the CMC group. However, the significantly high abundance of MDBOrad1_05282 (GH7) in the SD group did not lead to high CMCCase activity (Table S3 and Fig. S2a). It was speculated that this was due to the lack of expression of some endoglucanases, which assist CBHs by creating new chain ends on cellulose [52]. In addition, compared with the CMC group, all groups showed a comprehensive increase in the expression of MDBOrad1_01358 (GH5_9), where the enzyme abundance was quite low (0.012). This suggested the induction ability of natural carbon substrates on this enzyme.

4.2. Hemicellulose-degrading ability

Hemicelluloses, accounting for 20–35 % of the lignocellulosic biomass, are covalently linked to lignin and hydrogen-bonded to cellulose, creating complex frameworks that endow the cell wall with structural stability [55,56]. Hemicelluloses primarily consist of xylans, and their degradation requires the action of various enzymes, including xylanases, β -xylosidases, glucuronidases, α -L-arabinofuranosidases, and acetylxylan esterases [57]. In this study, xylanase activity was determined to indicate hemicellulose-degrading ability (Fig. 2d). Fungal xylanases are mainly classified into the GH10, GH11, and GH30 families in the CAZy database [58]. Among them, xylanases from the GH10 or GH11 family are the major xylan-degrading enzymes in nature, as reported in wild-type fungus *Fusarium oxysporum* and white-rot fungus *P. chrysosporium* [58,59]. In this study, the CMC group exhibited the highest xylanase activity, which was consistent with the fact that it had the highest abundance of the enzymes from GH10 and GH11 families encoding endo-1,4-beta-xylanase (Fig. S2b and Table S3). It has been proved that CMC effectively induces xylanase activity in *G. applanatum* [54]. The CC group had relatively high xylanase activity due to the corn cob substrate, rich in cellulose and xylan, effectively inducing xylanase production [60]. The SD and CH groups exhibited the lowest xylanase activity and were also clustered together (Fig. S1b), indicating weak xylanase induction by these two substrates in *O. raphanipes*.

4.3. Lignin-degrading ability

Lignin is the second most abundant component within lignocellulose. However, it reduces the efficiency of fungal fiber degradation by restricting the access of cellulolytic enzymes to cellulose and hemicellulose [61]. Therefore, disrupting the lignin structure is a crucial prerequisite for the effective utilization of lignocellulose. The primary enzymes playing crucial roles in lignin degradation can be sorted as lignin-modifying enzymes, which include laccases (belong to AA1), manganese peroxidases (MnPs), versatile peroxidases (VPs), and lignin peroxidases (LiPs) [26,62]. The latter three belong to the AA2 family and are considered key enzymes in lignin degradation as their encoding genes are exclusive to the genomes of white-rot fungi [62]. Additionally, companion enzymes co-expressed with peroxidases from the AA3, AA5, and AA7 families also participate in this process. Not all white-rot basidiomycetes possess identical ligninolytic enzyme systems. For example, genome sequencing of *P. ostreatus* revealed the absence of LiPs, along with the presence of three VPs and six MnPs [63,64]. In the secretome of *A. bisporus*, two MnPs were identified [30], while in the secretome of *O. raphanipes*, 12 laccases, one MnP3, and three VPs were detected.

In this study, the activities of laccase and MnP exhibited similar trends (Fig. S2c), suggesting a potential synergistic effect between them. In basidiomycetes such as *P. ostreatus* and *L. edodes*, which mainly degrade lignin during the mycelial growth phase, laccase, and peroxidase are of critical importance [65,66]. Similarly, in *A. bisporus* and *G. lucidum*, the expression of lignin-modifying enzymes was significantly higher during mycelial growth [67,68]. During the secretome assay of all groups, laccase-related proteins showed a high expression abundance, especially the laccase-2 encoded by MDBOrad1_21219, MDBOrad1_19878, and MDBOrad1_21230. Among these groups, the

CSL group had the highest abundance of laccases, followed by the Bran, Mix, CSK, and CC groups, while the CH and SD groups had the lowest. This finding was consistent with the results of the laccase enzyme activity assay (Fig. 2a). The efficient induction of laccase production by corn steep liquor, as observed in this study, has been previously documented in *P. ostreatus*, *Trametes versicolor*, and *Coriolopsis caperata* [69,70]. This can be due to the effect of the organic nitrogen source present in corn steep liquor. Notably, research has reported an inverse relationship between nitrogen demand and lignin-degrading enzymes [71]. Moreover, bran, also rich of nitrogen, has been identified as a favorable substrate for laccase production in *C. caperata* and *Cerrena unicolor* [70,72]. Furthermore, it is worth noting that, except for the CSL group, the MnP activities in all groups were relatively lower compared to the laccase activities (Fig. 2b). Additionally, the expression abundance of all identified proteins belonging to the AA2 family was insignificant (Fig. S2d). One possible reason could be that only a single protein, MDBOrad1_13453, encoding MnP3 (with a notably low abundance across all groups) was identified in the secretome of *O. raphanipes*. Another possible explanation might be related to the developmental stage, as studies on *G. lucidum* and *P. eryngii* have shown that laccase activity peaked during the mycelial growth stage, while MnP activity reached its maximum during primordia formation [31,73].

4.4. Amylase

Amylase can degrade the starch in nutritive substances like wheat bran, enabling the prior utilization of starch over other polysaccharides in the medium [65]. Through continuous enzyme activity assays, it was evident that *O. raphanipes* exhibited relatively strong amylase activity across all groups, with high amylase activity obtained from the early stage of mycelium cultivation (Fig. 2e). This was consistent with the result obtained from *M. importuna* when grown on different carbon sources [27]. Alpha-amylases are primarily categorized into four families: GH13, GH57, GH119, and GH126 [74]. Among these, the GH13 family is recognized as one of the key enzyme families involved in starch metabolism [75]. In the secretome of *O. raphanipes*, only the proteins from the GH13 subfamily (GH13_1 and GH13_32) were detected (Table S3). Notably, three or more proteins within the GH13 family had undetectable expression abundances in the CH, CSK, and SD groups, which may explain the relatively low enzyme activities observed in these groups (Table S3). In contrast to this result, in *L. edodes*, the alpha-amylase (GH13) was significantly upregulated in the hyphal transcriptional response to the cornstalk substrate [76]. This indicated the differences in amylase induction by the same substrate between these two fungal species.

4.5. Pectinase

Pectin, a highly branched structural heteropolysaccharide, requires a broad array of enzymes for its degradation. Pectinase, in particular, is commonly used to biochemically decompose pectin-rich lignocellulosic waste biomass. In this study, 33 pectinases were identified from the eight proteomes (Table S3 and Fig. S2f). Among these, the most abundant pectinase enzymes were pectate lyases (classified as PL1_2, PL1_7, PL3_2, and PL9_3), with the highest abundance observed in the CC and SD groups. Four alpha-L-mannosidase (GH78) and seven enzymes belonging to GH105 were identified, with differential expression abundance among different groups. A certain relationship between the expression abundance of pectinase-related proteins and mycelium growth was observed in this study. For example, the bran and CC groups, with high expression of most pectinase-related proteins, also showed better mycelium growth. Conversely, the CMC group had notably low pectinase expression and poor mycelium growth. In the CSK group, over half of the pectinase-related proteins had undetectable abundance, corresponding to low mycelium dry weight. The solubilization of pectin could enhance the accessibility of microorganisms and enzymes, thereby

facilitating the decomposition of lignocellulose [76]. Previous studies have revealed that different *Pleurotus* species with more pectinase enzyme produced could degrade the pectin and yield more mycelium [77].

4.6. Growth comparison of different substrates

The growth and development of edible fungi are intricately influenced by the cultivation substrate, which serves as the primary source of nutrients and environmental cues. Thus, choosing an appropriate cultivation substrate for edible fungi is crucial. When fungal species grow on plant-based materials, the genes and proteins they express reflect their unique lifestyle and specific lignocellulose conversion strategies. In this study, we employed Kirk's liquid medium supplemented with eight different carbon sources. As expected, substrates rich in lignin were found to stimulate the expression of cellulase and hemicellulase in *O. raphanipes*. Among the tested substrates, the Bran group exhibited a significant advantage in mycelium growth and dry weight. This group also exhibited notably high activities of amylase, laccase, and cellulase. Wheat bran has long been recognized as an excellent substrate for cultivating many mushroom species [70]. For instance, *Macrocybe esculenta* cultured on the bran-based medium achieved maximum biomass along with high activities of endoglucanase, β -glucosidase, amylase, and laccase [78]. Similarly, when *Pleurotus* spp. and *L. edodes* were grown on various agricultural wastes, adding rice bran increased the biological efficiency [53]. This higher enzyme activity in these bran-based cultures might be due to the enhanced availability of monosaccharides, polysaccharides, or nitrogen sources. These findings emphasized the importance of optimizing the C/N ratio of the lignocellulosic residues by adding nitrogen sources for mushroom cultivation. Beyond bran, *O. raphanipes* mycelium also thrived on a medium supplemented with cottonseed hulls. This observation was consistent with the previous cultivation studies on *O. canarii*, where a substrate composed of 80 % cottonseed hull and 18 % wheat bran was identified as the optimal growth condition after considering multiple factors [49]. RDA provided evidence that *O. raphanipes* could efficiently utilize cellulose, as indicated by the relatively minor impact of CMCase activity on the secretomes of different groups. In the CSL group, the absence of solid matrixes prevented the mycelium from expanding on the surface. As a result, the mycelium grew in a submerged manner. Given the relatively high nitrogen content in corn steep liquor, this might have contributed to the significantly higher activities of laccase and MnP in this group (Fig. 2). Concurrently, the number of secreted proteins identified in this group was the lowest among all groups (Fig. 3). In contrast, when cultured in the lignin-rich sawdust medium, the mycelium formed a thin layer on the liquid surface, resulting in extremely low dry weight and protein content. This phenomenon can be attributed to the complex structure of lignin, which impedes the mycelium's access to utilize the cellulose and hemicellulose components within the substrate. These results indicated that the sawdust had a limited capacity to induce lignin-degrading enzymes in *O. raphanipes*. The CSK group exhibited the greatest quality of secreted proteins, particularly those associated with oxidoreductase and protease & peptidase. Nevertheless, this group also showed the largest number of down-regulation proteins, which might be one of the factors contributing to the less vigorous growth of the mycelium. Finally, the RDA results revealed that the activities of laccase, MnP, and xylanase induced by different substrates had the most substantial effects on the expression of the secretome proteins, highlighting the key role of these enzymes in the substrate-mediated regulation of fungal cultivation.

5. Conclusions

This study systematically elucidated the lignocellulose degradation mechanism of *O. raphanipes* across eight different lignocellulosic biomasses, demonstrating significant metabolic plasticity in response to

- [24] A. Trochine, N. Bellora, P. Nizovoy, R. Duran, G. Greif, V. de Garcia, C. Batthyany, C. Robello, D. Libkind, Genomic and proteomic analysis of *Tausonia pullulans* reveals a key role for a GH15 glucoamylase in starch hydrolysis, *Appl. Microbiol. Biotechnol.* 106 (12) (2022) 4655–4667, <https://doi.org/10.1007/s00253-022-12025-7>.
- [25] M. Alfaro, J.A. Oguiza, L. Ramirez, A.G. Pisabarro, Comparative analysis of secretomes in basidiomycete fungi, *J. Proteome* 102 (2014) 28–43, <https://doi.org/10.1016/j.jprotp.2014.03.001>.
- [26] G. Liu, L. Zhang, X. Wei, G. Zou, Y. Qin, L. Ma, J. Li, H. Zheng, S. Wang, C. Wang, L. Xun, G.P. Zhao, Z. Zhou, Y. Qu, Genomic and secretomic analyses reveal unique features of the lignocellulolytic enzyme system of *Penicillium decumbens*, *PLoS One* 8 (2) (2013) e55185, <https://doi.org/10.1371/journal.pone.0055185>.
- [27] Y. Cai, X. Ma, Q. Zhang, F. Yu, Q. Zhao, W. Huang, J. Song, W. Liu, Physiological characteristics and comparative secretome analysis of *Morchella importuna* grown on glucose, rice straw, sawdust, wheat grain, and mix substrates, *Front. Microbiol.* 12 (2021) 636344, <https://doi.org/10.3389/fmicb.2021.636344>.
- [28] F. Valadares, T.A. Goncalves, A. Damasio, A.M. Milagres, F.M. Squina, F. Segato, A. Ferraz, The secretome of two representative lignocellulose-decay basidiomycetes growing on sugarcane bagasse solid-state cultures, *Enzym. Microb. Technol.* 130 (2019) 109370, <https://doi.org/10.1016/j.enzymictec.2019.109370>.
- [29] Z. Li, C. Zhao, Y. Zhou, S. Zheng, Q. Hu, Y. Zou, Label-free comparative proteomic analysis of *Pleurotus eryngii* grown on sawdust, bagasse, and peanut shell substrates, *J. Proteome* 294 (2024) 105074, <https://doi.org/10.1016/j.jprotp.2024.105074>.
- [30] K. Duran, J. Magnin, A.H.P. America, M. Peng, R. Hilgers, R.P. de Vries, J.J. P. Baars, W.J.H. van Berkel, T.W. Kuyper, M.A. Kabel, The secretome of *Agaricus bisporus*: temporal dynamics of plant polysaccharides and lignin degradation, *iScience* 26 (7) (2023) 107087, <https://doi.org/10.1016/j.isci.2023.107087>.
- [31] P. Wang, X. Feng, Z. Lv, J. Liu, Q. Teng, T. Chen, Q. Liu, Temporal dynamics of lignin degradation in *Quercus acutissima* sawdust during *Ganoderma lucidum* cultivation, *Int. J. Biol. Macromol.* 268 (Pt 1) (2024) 131686, <https://doi.org/10.1016/j.ijbiomac.2024.131686>.
- [32] Q. Xiao, F. Ma, Y. Li, H. Yu, C. Li, X. Zhang, Differential proteomic profiles of *pleurotus ostreatus* in response to lignocellulosic components provide insights into divergent adaptive mechanisms, *Front. Microbiol.* 8 (2017) 480, <https://doi.org/10.3389/fmicb.2017.00480>.
- [33] S. Gomathy, R. Sridharan, P.S. Kumar, V.G. Krishnaswamy, D.A.A. Farraj, S. Chen, Application of alkaline MnP immobilized Luffa fibers in mixed azo dyes degradation, *Environ. Technol. Innov.* 24 (2021) 101964, <https://doi.org/10.1016/j.eti.2021.101964>.
- [34] T.K. Ghose, Measurement of cellulase activities, *IUPAC Standards Online* 59 (2016) 257–268, <https://doi.org/10.1515/iupac.59.0006>.
- [35] M. Bailey, P. Biely, K. Poutanen, Interlaboratory testing of methods for assay of xylanase activity, *J. Biotechnol.* 23 (3) (1992) 257–270, [https://doi.org/10.1016/0168-1656\(92\)90074-j](https://doi.org/10.1016/0168-1656(92)90074-j).
- [36] A. Aygan, B. Arkan, H. Korkmaz, S. Dinçer, O. Colak, Highly thermostable and alkaline α -amylase from a halotolerant-alkaliphilic *Bacillus* sp. AB68, *Braz. J. Microbiol.* 39 (3) (2008) 547–553, <https://doi.org/10.1590/S1517-838220080003000027>.
- [37] T. Isaacson, C.M. Damasceno, R.S. Saravanan, Y. He, C. Catalá, M. Saladié, J. K. Rose, Sample extraction techniques for enhanced proteomic analysis of plant tissues, *Nat. Protoc.* 1 (2) (2006) 769–774, <https://doi.org/10.1038/nprot.2006.102>.
- [38] L. Xu, W. Yang, T. Qiu, X. Gao, H. Zhang, S. Zhang, H. Cui, L. Guo, H. Yu, H. Yu, Complete genome sequences and comparative secretomic analysis for the industrially cultivated edible mushroom *Lyophyllum decastes* reveals insights on evolution and lignocellulose degradation potential, *Front. Microbiol.* 14 (2023) 1137162, <https://doi.org/10.3389/fmicb.2023.1137162>.
- [39] L. Zhu, Y. Su, S. Ma, L. Guo, S. Yang, H. Yu, Comparative proteomic analysis reveals candidate pathways related to the effect of different light qualities on the development of mycelium and fruiting body of *Pleurotus ostreatus*, *J. Agric. Food Chem.* 72 (2) (2024) 1361–1375, <https://doi.org/10.1021/acs.jafc.3c06083>.
- [40] M. Kanehisa, S. Goto, Y. Sato, M. Furumichi, M. Tanabe, KEGG for integration and interpretation of large-scale molecular data sets, *Nucleic Acids Res.* 40 (Database issue) (2012) D109–D114, <https://doi.org/10.1093/nar/gkr988>.
- [41] T.N. Petersen, S. Brunak, G. von Heijne, H. Nielsen, SignalP 4.0: discriminating signal peptides from transmembrane regions, *Nat. Methods* 8 (10) (2011) 785–786, <https://doi.org/10.1038/nmeth.1701>.
- [42] T. Kijpornyongpan, A. Schwartz, A. Yaguchi, D. Salvachua, Systems biology-guided understanding of white-rot fungi for biotechnological applications: a review, *iScience* 25 (7) (2022) 104640, <https://doi.org/10.1016/j.isci.2022.104640>.
- [43] H. Kobori, J. Wu, H. Takemura, J.H. Choi, N. Tada, H. Kawagishi, Utilization of corn steep liquor for the production of fairy chemicals by *Lepista sordida* mycelia, *J. Fungi* 8 (12) (2022) 1269, <https://doi.org/10.3390/jof8121269>.
- [44] J.R. Wisniewski, A. Zougman, N. Nagaraj, M. Mann, Universal sample preparation method for proteome analysis, *Nat. Methods* 6 (5) (2009) 359–362, <https://doi.org/10.1038/nmeth.1322>.
- [45] V.A. Duong, H. Lee, Bottom-up proteomics: advancements in sample preparation, *Int. J. Mol. Sci.* 24 (6) (2023) 5350, <https://doi.org/10.3390/ijms24065350>.
- [46] H.V. Scheller, P. Ulvskov, Hemicelluloses, *Annu. Rev. Plant Biol.* 61 (2010) 263–289, <https://doi.org/10.1146/annurev-arplant-042809-112315>.
- [47] P.J. Smith, H.T. Wang, W.S. York, M.J. Peña, B.R. Urbanowicz, Designer biomass for next-generation biorefineries: leveraging recent insights into xylan structure and biosynthesis, *Biotechnol. Biofuels* 10 (2017) 286, <https://doi.org/10.1186/s13068-017-0973-z>.
- [48] M.S. Doblin, F. Pettolino, A. Bacic, Plant cell walls: the skeleton of the plant world, *Funct. Plant Biol.* 37 (5) (2010) 357–381, <https://doi.org/10.1071/fp09279>.
- [49] F. Xu, Z. Li, Y. Liu, C. Rong, S. Wang, Evaluation of edible mushroom *Oudemansiella canarii* cultivation on different lignocellulosic substrates, *Saudi J. Biol. Sci.* 23 (5) (2016) 607–613, <https://doi.org/10.1016/j.sjbs.2015.07.001>.
- [50] F.J. Ruiz-Duenas, J.M. Barrasa, M. Sánchez-García, S. Camarero, S. Miyauchi, A. Serrano, D. Linde, R. Babiker, E. Drula, I. Ayuso-Fernández, R. Pacheco, G. Padilla, P. Ferreira, J. Barriuso, H. Kellner, R. Castanera, M. Alfaro, L. Ramirez, A.G. Pisabarro, R. Riley, A. Kuo, W. Andreopoulos, K. LaButti, J. Pangilinan, A. Tritt, A. Lipzen, G. He, M. Yan, V. Ng, I.V. Grigoriev, D. Cullen, F. Martin, M. N. Rosso, B. Henrissat, D. Hibbett, A.T. Martínez, Genomic analysis enlightens agaricales lifestyle evolution and increasing peroxidase diversity, *Mol. Biol. Evol.* 38 (4) (2021) 1428–1446, <https://doi.org/10.1093/molbev/msaa301>.
- [51] J.V. Vermaas, M.F. Crowley, G.T. Beckham, C.M. Payne, Effects of lytic polysaccharide monoxygenase oxidation on cellulose structure and binding of oxidized cellulose oligomers to cellulases, *J. Phys. Chem. B* 119 (20) (2015) 6129–6143, <https://doi.org/10.1021/acs.jpcc.5b00778>.
- [52] M. Kurasin, P. Valjamae, Processivity of cellobiohydrolases is limited by the substrate, *J. Biol. Chem.* 286 (1) (2011) 169–177, <https://doi.org/10.1074/jbc.M110.161059>.
- [53] J.M. da Luz, M.D. Nunes, S.A. Paes, D.P. Torres, M. de Cassia Soares, M.C. Kasuya da Silva, Lignocellulolytic enzyme production of *Pleurotus ostreatus* growth in agroindustrial wastes, *Braz. J. Microbiol.* 43 (4) (2012) 1508–1515, <https://doi.org/10.1590/S1517-838220120004000035>.
- [54] D.N. Salmon, M.R. Spier, C.R. Soccol, L.P. Vandenberghe, V. Weingartner Montibeller, M.C. Bier, V. Faraco, Analysis of inducers of xylanase and cellulase activities production by *Ganoderma applanatum* LPB MR-56, *Fungal Biol.* 118 (8) (2014) 655–662, <https://doi.org/10.1016/j.funbio.2014.04.003>.
- [55] B. Ordóñez-Arevalo, E. Huerta-Lwanga, M.L.A. Calixto-Romo, M.F. Dunn, K. Guillen-Navarro, Hemicellulolytic bacteria in the anterior intestine of the earthworm *Eisenia fetida* (Sav.), *Sci. Total Environ.* 806 (Pt 4) (2022) 151221, <https://doi.org/10.1016/j.scitotenv.2021.151221>.
- [56] J. Broeker, M. Mechelke, M. Baudrexel, D. Mennerich, D. Hornburg, M. Mann, W. H. Schwarz, W. Liebl, V.V. Zverlov, The hemicellulose-degrading enzyme system of the thermophilic bacterium *Clostridium stercorarium*: comparative characterisation and addition of new hemicellulolytic glycoside hydrolases, *Biotechnol. Biofuels* 11 (2018) 229, <https://doi.org/10.1186/s13068-018-1228-3>.
- [57] R. Kumar, S. Singh, O.V. Singh, Bioconversion of lignocellulosic biomass: biochemical and molecular perspectives, *J. Ind. Microbiol. Biotechnol.* 35 (5) (2008) 377–391, <https://doi.org/10.1007/s10295-008-0327-8>.
- [58] K. Kojima, N. Sunagawa, Y. Yoshimi, T. Tryfona, M. Samejima, P. Dupree, K. Igarashi, Acetylated xylan degradation by glycoside hydrolase family 10 and 11 xylanases from the white-rot fungus *Phanerochaete chrysosporium*, *J. Appl. Glycosci.* 69 (2) (2022) 35–43, <https://doi.org/10.5458/jag.jag.JAG-2021.0017>.
- [59] Y. Huang, P.K. Busk, L. Lange, Cellulose and hemicellulose-degrading enzymes in *Fusarium commune* transcriptome and functional characterization of three identified xylanases, *Enzym. Microb. Technol.* 73-74 (2015) 9–19, <https://doi.org/10.1016/j.enzymictec.2015.03.001>.
- [60] W. Mardones, E. Callegari, J. Eyzaguirre, Corncob and sugar beet pulp induce specific sets of lignocellulolytic enzymes in *Penicillium purpurogenum*, *Mycology* 10 (2) (2018) 118–125, <https://doi.org/10.1080/21501203.2018.1517830>.
- [61] L. Kumar, V. Arantes, R. Chandra, J. Saddler, The lignin present in steam pretreated softwood binds enzymes and limits cellulose accessibility, *Bioresour. Technol.* 103 (1) (2012) 201–208, <https://doi.org/10.1016/j.biortech.2011.09.091>.
- [62] T. Nakazawa, I. Yamaguchi, Y. Zhang, C. Saka, H. Wu, K. Kayama, M. Kawachi, M. Sakamoto, Y. Honda, Experimental evidence that lignin-modifying enzymes are essential for degrading plant cell wall lignin by *Pleurotus ostreatus* using CRISPR/Cas9, *Environ. Microbiol.* 25 (10) (2023) 1909–1924, <https://doi.org/10.1111/1462-2920.16427>.
- [63] D. Knop, O. Yarden, Y. Hadar, The ligninolytic peroxidases in the genus *Pleurotus*: divergence in activities, expression, and potential applications, *Appl. Microbiol. Biotechnol.* 99 (3) (2015) 1025–1038, <https://doi.org/10.1007/s00253-014-6256-8>.
- [64] E. Fernandez-Fueyo, F.J. Ruiz-Duenas, M.J. Martinez, A. Romero, K.E. Hammel, F. J. Medrano, A.T. Martinez, Ligninolytic peroxidase genes in the oyster mushroom genome: heterologous expression, molecular structure, catalytic and stability properties, and lignin-degrading ability, *Biotechnol. Biofuels* 7 (1) (2014) 2, <https://doi.org/10.1186/1754-6834-7-2>.
- [65] N. Kobayashi, N. Wada, H. Yokoyama, Y. Tanaka, T. Suzuki, N. Habu, N. Konno, Extracellular enzymes secreted in the mycelial block of *Lentinula edodes* during hyphal growth, *AMB Express* 13 (1) (2023) 36, <https://doi.org/10.1186/s13568-023-01547-6>.
- [66] V. Elisashvili, E. Kachlishvili, M.J. Penninckx, Lignocellulolytic enzymes profile during growth and fruiting of *Pleurotus ostreatus* on wheat straw and tree leaves, *Acta Microbiol. Immunol. Hung.* 55 (2) (2008) 157–168, <https://doi.org/10.1556/AMicr.55.2008.2.7>.
- [67] M.V.A. Pontes, A. Patyshakuliyeva, H. Post, E. Jurak, K. Hilden, M. Altelaar, A. Heck, M.A. Kabel, R.P. de Vries, M.R. Makela, The physiology of *Agaricus bisporus* in semi-commercial compost cultivation appears to be highly conserved among unrelated isolates, *Fungal Genet. Biol.* 112 (2018) 12–20, <https://doi.org/10.1016/j.fgb.2017.12.004>.
- [68] S. Zhou, J. Zhang, F. Ma, C. Tang, Q. Tang, X. Zhang, Investigation of lignocellulolytic enzymes during different growth phases of *Ganoderma lucidum* strain G0119 using genomic, transcriptomic and secretomic analyses, *PLoS One* 13 (5) (2018) e0198404, <https://doi.org/10.1371/journal.pone.0198404>.

- [69] F. Wang, J.H. Hu, C. Guo, C.Z. Liu, Enhanced laccase production by *Trametes versicolor* using corn steep liquor as both nitrogen source and inducer, *Bioresour. Technol.* 166 (2014) 602–605, <https://doi.org/10.1016/j.biortech.2014.05.068>.
- [70] P. Nandal, S.R. Ravella, R.C. Kuhad, Laccase production by *Coriopsis caperata* RCK2011: optimization under solid state fermentation by Taguchi DOE methodology, *Sci. Rep.* 3 (2013) 1386, <https://doi.org/10.1038/srep01386>.
- [71] V.P. Kumar, M. Sridhar, S.A. Kumar, R. Bhatta, Elucidating the role of media nitrogen in augmenting the production of lignin-depolymerizing enzymes by white-rot fungi, *Microbiol. Spectr.* 11 (5) (2023) e0141923, <https://doi.org/10.1128/spectrum.01419-23>.
- [72] V. Elisashvili, E. Kachlishvili, Physiological regulation of laccase and manganese peroxidase production by white-rot *Basidiomycetes*, *J. Biotechnol.* 144 (1) (2009) 37–42, <https://doi.org/10.1016/j.jbiotec.2009.06.020>.
- [73] T.T. Ni, X. Zhao, Z. Xing, Q. Tan, J.A. Buswell, Ligno(hemi)cellulolytic enzyme profiles during the developmental cycle of the royal oyster medicinal mushroom *Pleurotus eryngii* (Agaricomycetes) grown on supplemented Agri-wastes, *Int. J. Med. Mushrooms* 22 (9) (2020) 919–929, <https://doi.org/10.1615/IntJMedMushrooms.2020035958>.
- [74] M. Martinovicova, S. Janecek, In silico analysis of the alpha-amylase family GH57: eventual subfamilies reflecting enzyme specificities, *3 Biotech.* 8 (7) (2018) 307, <https://doi.org/10.1007/s13205-018-1325-9>.
- [75] Y. Miyasaka, K. Yokoyama, T. Kozono, Y. Kitano, T. Miyazaki, M. Sakaguchi, A. Nishikawa, T. Tonozuka, Structural basis for the recognition of alpha-1,6-branched alpha-glucan by GH13_47 alpha-amylase from *Rhodothermus marinus*, *Proteins* 92 (8) (2024) 984–997, <https://doi.org/10.1002/prot.26695>.
- [76] C. Mou, Y. Gong, L. Chen, F. Martin, H. Kang, Y. Bian, Comparative analysis of simulated in-situ colonization and degradation by *Lentinula edodes* on oak wafer and corn stalk, *Front. Microbiol.* 14 (2003) 1286064, <https://doi.org/10.3389/fmicb.2023.1286064>.
- [77] G. Dissasa, Cultivation of different oyster mushroom (*Pleurotus* species) on coffee waste and determination of their relative biological efficiency and pectinase enzyme production, Ethiopia, *Int. J. Microbiol.* 2022 (2022) 5219939, <https://doi.org/10.1155/2022/5219939>.
- [78] L. Papinutti, B. Lechner, Influence of the carbon source on the growth and lignocellulolytic enzyme production by *Morchella esculenta* strains, *J. Ind. Microbiol. Biotechnol.* 35 (12) (2008) 1715–1721, <https://doi.org/10.1007/s10295-008-0464-0>.